Korean J. Chem. Eng., 33(8), 2439-2452 (2016)
DOI: 10.1007/s11814-016-0107-5

pISSN: 0256-1115
eISSN: 1975-7220

Sulfonation and mixing with TiO_2 nanoparticles as two simultaneous solutions for reducing fouling of polysulfone loose nanofiltration membrane

Ahmad Akbari*,† and Maryam Homayoonfal**

*Institute of Nanoscience and Nanotechnology, University of Kashan, Kashan, Iran
**Department of Chemical Engineering, College of Engineering, University of Isfahan, P. O. Box 81746-73441, Isfahan, Iran
(*Received 12 December 2015 • accepted 19 April 2016*)

Abstract−The aim of this research is synthesis of high performance loose nanofiltration membranes for separation of direct dyes from textile wastewater. This involved sulfonation of polysulfone with the aim of increasing hydrophilicity and permeability; synthesis of a sulfonated polysulfone and polysulfone (SPSf/PSf) blended membrane for developing the mechanical resistance and stability of the filtration behavior; and synthesis of TiO_2/SPSf/PSf nanocomposite membrane for magnifying selectivity. FTIR analysis confirmed the sulfonated groups and the TiO_2 nanoparticles presence. AFM and SEM analysis proved the highest surface roughness and the smallest pore size of TiO_2/SPSf/PSf nanocomposite membrane, respectively. The results of water absorption test revealed that the highest level of hydrophilicity belonged to the SPSf/PSf followed by TiO_2/SPSf/PSf membrane. The nanofiltration tests showed that the SPSf/PSf membranes enjoy the highest permeability, while the TiO_2/SPSf/PSf nanocomposite not only had an acceptable permeability but also presented the highest dye separation efficiency.

Keywords: Textile Wastewater, Loose Nanofiltration, Sulfonated Polysulfone, Nanocomposite Membrane, TiO_2 Nanoparticle

INTRODUCTION

Textile wastewater is one of the major environmental pollutants, the treatment of which has attracted a great deal of attention in recent years [1]. There are different methods for separating various types of dyes including membrane filtration [2]. Considering the size of textile direct dyes, the nanofiltration process is effective for separation of these substances from wastewater [3-5]. Based on the reports by different researchers, the nanofiltration process has the potential to separate dyes with a yield over 90% [1,6-8]. However, one of the main problems of nanofiltration process during the treatment of textile wastewater is membrane fouling [3,8,9]. According to many reports, membrane fouling is directly related to the hydrophobicity of the membrane surface [10-12], generally due to absorption of nonpolar solutes, hydrophobic particles or bacteria on the membrane surface [13]. There are different methods for reducing membrane fouling that might be based on modification of the membrane structure or modification of the nanofiltration process [14]. To reduce hydrophobicity and in turn the membrane fouling, the strategies based on membrane modification might rely on modification of the polymer prior to membrane synthesis or surface modification of pre-synthesized membrane [15,16]. Based on different studies, the modification of the polymer has a higher effectiveness in reducing fouling when compared to the surface modification of membrane [17]. One of the key methods of membrane modification is co-polymerization using hydrophilic monomers [16,18,19]. The hydrophilic functional groups in this method can be hydroxyl, amine, carboxyl, and sulfone groups [20,21]. In addition to the possibility of copolymerization with hydrophilic monomers, blending hydrophilic minerals into membrane substrate is also a common method in mitigating membrane fouling [18]. One of the hydrophilic minerals that has attracted a great deal of attention regarding developing permeability is metal and metal oxide nanoparticles [22-24]. It is expected that concurrent use of these two mentioned methods (i.e. copolymerization with hydrophilic monomers and blending with nano-structures) has a huge effect on increasing permeability and diminishing the level of membrane fouling [25-27].

In this research, high permeability, low pressure drop polysulfone loose nanofiltration membrane [7,28,29] was used to separate a sample of direct dyes from textile wastewater. Too elevate membrane permeability, avoid fouling, and considering presence of sulfonated groups within the structure of direct dyes (which enhances repulsion between dye molecule and the surface of sulfonated membrane), the membrane substance was co-polymerized with sulfonated polysulfone. In this way, the SPSf/PSf membrane enjoyed high permeability and at the same time prevented from sedimentation of dyes on the membrane surface. With the aim of maintaining permeability and to elevate the level of membrane selectivity and considering the hydrophilicity, the mechanical resistance of TiO_2 nanoparticles, the combination of these nanoparticles with the SPSf/PSf blended membrane was utilized. Four main steps were taken in this research: sulfonation of polysulfone, synthesis of the SPSf/PSf blended membrane, synthesis of the TiO_2/SPSf/PSf nanocomposite membrane, and comparison of the structure and nanofiltration performance of the synthesized membranes for removal of textile dyes. Note that the best membrane synthesized in each stage entered the next stage for further modification. Finally, using FTIR, AFM, SEM, and MWCO, water absorption, permeability, and separation

†To whom correspondence should be addressed.
E-mail: Akbari@kashanu.ac.ir

of the saline solution analyses, the best membrane sample was introduced for the treatment of textile wastewater.

MATERIALS AND METHODS

This research consists of four main stages. It is expected that at the end it culminates in synthesis of loose nanofiltration membranes with fine quality. These stages are:

1. Synthesis of sulfonated polysulfone and selection of the optimal sulfonation degree.
2. Application of SPSf with optimal sulfonation degree for synthesis of the SPSf/PSf blended membrane and determination of the optimal weight ratio of SPSf/PSf.
3. Application of the optimal weight ratio of SPSf/PSf for synthesizing membrane at different concentrations of polymer and various temperatures of coagulation bath and selection of the optimal membrane.
4. Investigation of the effect of TiO_2 nanoparticles addition to the optimal membrane prepared in the previous stage on specification of the optimal concentration of the titania nanoparticles.

Each of these stages is further explained in the following sections.

1. Materials and Equipment

Table 1 lists the materials and equipment utilized in this research.

2. Methods

2-1. Synthesis of the Sulfonated Polysulfone

To synthesize sulfonated polysulfone, first polysulfone was dried for 48 hours in an oven at 120 °C. It was then dissolved in chloroform solvent with a ratio of 1 : 10 at 250 rpm stirring to achieve a totally clear solution. In the PSf sulfonation reaction, there are various effective parameters including the concentration of the sulfonation agent, time, and temperature [30]. Temperature growth causes significant reduction of synthesis time, on the one hand, and results in increased dissociation of the PSf chains, on the other hand [30,31]. Breakdown of PSf chains leads to declined molecular weight and in turn further swelling of the membrane film. Accordingly, in line with the synthesis method reported by other researchers, the environment temperature was chosen for the reaction [32]. The concentration of the sulfonation agent and time are two parallel parameters. Thus, the concentration of sulfonation agent (molar ratio of the sulfonation agent to the number of polymer repetition units) was considered constant. The effect of time (1, 3, 6, 12, 24, and 48 hours) on sulfonation degree was further examined. The sulfonation agent, TMSC1S was added to the solution dropwise and within a 15-minute period in order for the sulfonation reaction to be carried out through the mechanism presented in Fig. 1.

Table 1. The list of materials and equipment used in this research

Material		
Chemical	Properties	Supplier
Polysulfone	MW: 35000 Da	Across Organics
N-methylpyrrolidone		Merck
Polyethylene glycol	MW: 3000, 6000, 10000 Da	Merck
Potassium hexacyanoferrate (iii)		Merck
Trimethylsilyl chlorosulfonate (TMSClS)		Merck
HCl, NaOH		Merck
Methanol, Ethanol, Chloroform		Merck
ammonium hydroxide		Merck
sodium methoxide		Merck
Na_2SO_4		Merck
$BaCl_2$, KI, I_2		Merck
Direct yellow 12	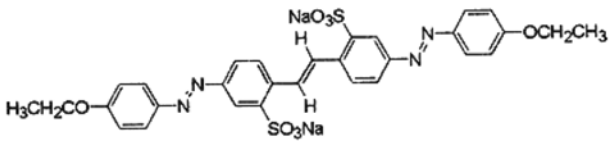	Rang Alvan Sabet
Deionized water		
Instrument		
Analysis	Model	Supplier
Spectrophotometer	GBC, Cintra 101	Australia
Conductometer	WTW inoLab Cond 720	Germany
FT-IR	Shimadzu Varian	Japan
SEM	KYKY-EM 3200	China
AFM	Nanoscope	USA
Ultrasonic Cleaner	Elma EG 30/H	Germany
Casting Knife, Cross flow filtration		

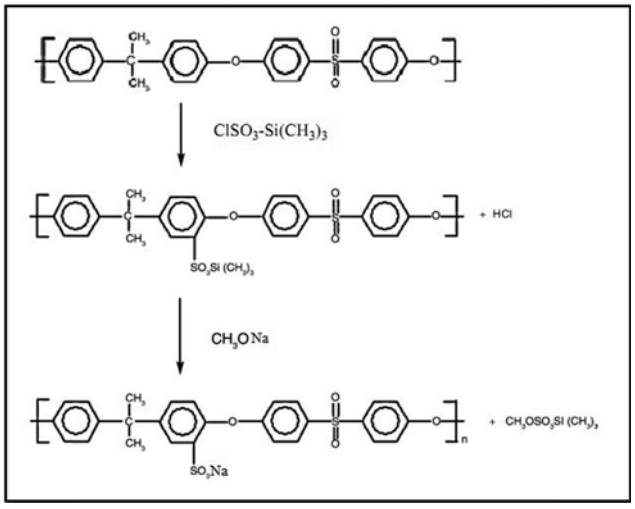

Fig. 1. PSf sulfonation reaction.

After passage of the desired time, sodium methoxide solution 30 w% prepared in methanol was gradually added to the sulfonation reaction solution. To expel the trimethylsilane groups completely, additional amount of sodium methoxide solution was further added to the solution to ensure the complete discharge of these substances from the reaction medium. After one hour, direction was completed after which the reaction solution was added to the ethanol bath dropwise. Since ethanol is considered non-solvent for the polymer, SPSf immediately sediments in the bath, where the impurities, byproducts of the reaction, and excessive amounts of sodium methoxide are dissolved in the ethanol and leave the polymer. Next, the sulfonated polymer was washed with water and ethanol so that trivial amounts of the remaining impurities also leave the polymer. At the end, the polymer was dried for 48 hours in an oven at 120 °C [30-32].

2-2. Preparation of the Sulfonated Polysulfone Membrane

SPSf polymer prepared in the previous stage was used with different sulfonation degrees (9.4, 45.3, 67.1, 77, and 95.1) and different weight percentages (25 and 30 wt%) for synthesis of the membrane. The desired weights of SPSf were accurately weighed together with NMP solvent. Using liquid paraffin bath, a homogeneous solution was synthesized at 90 °C within six hours. Thereafter, the solution was film-dragged on the glass using a casting knife and placed in coagulation bath (distilled water) immediately.

2-3. Preparation of the Polysulfone/Sulfonated Polysulfone Blended Membranes

The PSf and SPSf blended membrane was next prepared by phase inversion method. First a certain amount of both polymers with a specific SPSf/PSf weight ratio (10/90, 20/80, 30/70, 40/60, and 50/50) was weighed carefully. They were then added gradually to the NMP solution (75% wt%). To achieve an impeccable membrane (pucker, shrinkage, perforation, and leakage) it is required that the polymer solution be totally homogeneous and devoid of any impurities and bubbles.

After these, the polymer solution previously placed inside the paraffin bath at 90 °C, was placed on a magnetic stirrer for 12 hours. To obtain a more homogeneous solution, it was put inside an ultrasonic bath under sound waves for two minutes. Once the solution was fully clear and homogeneous, it was given time to expel its bubbles in a stationary position. Presence of bubbles in the casting solution results in perforation of the membrane [33,34].

After preparation of the solution, using a casting knife of 5 cm wide, a polymer film layer 200 μm thick was casted onto the fully smooth surface of the glass and was further placed inside in a coagulation bath. The obtained membrane remained in this bath for 12 hours so that its morphology fully stabilized while the solvent and additives were fully discharged off the membrane. The obtained membranes were cut in suitable sizes (4 * 8 cm) and were employed in a filtration device for evaluation. After determination of the optimal ratio of SPSf/PSf, the effect of two parameters, i.e., the polymer concentration (26, 28, 30, 32 wt%) and the temperature of coagulation bath (5, 15, 25 °C) on the structure and properties of the membrane, was investigated to achieve a loose nanofiltration membrane with desirable properties.

2-4. Preparation of TiO_2/SPSf/PSf Blend Membrane

To maintain the level of permeability, increase mechanical resistance, and develop the membrane selectivity, titania nanoparticles were chosen to be added to the membrane structure thanks to their good adaptability with organic solvents for preparation of PSf casting solutions. At this stage, titanium dioxide nanoparticles with a size of 25 nm with weight percentages of 0.01, 0.05, and 0.1 were added to the polymer solution containing the optimal ratio of polysulfone and sulfonated polysulfone. Next, the nanocomposite membrane containing titania was prepared using phase inversion method previously described. The membranes synthesized at this stage were carefully evaluated in a filtration device.

2-5. Evaluation of the Membrane Performance

The performance of membranes synthesized in a cross flow cell was evaluated at operational pressure of 4 bar, feed rate of 5 L/min, and temperature of 25±2 °C. The factors accounting for the membrane performance considered in this research include measurement of the pure water flux, molecular weight cut off (MWCO) (MWCO), salt rejection, and dye rejection.

$$J_w = \frac{\Delta W}{A \times \Delta t} \quad (1)$$

where, ΔW is the volume of the solution passing through the membrane (m^3), A is the effective membrane area (m^2), and Δt is the time it takes for the solution to pass through the membrane (h).

Molecular weight cut off (MWCO) of membranes is an indirect criterion of the diameter of the pores. It is the molecular weight of the smallest macromolecule rejected by the membrane under certain operational circumstances as much as 90-95%. In this research, the macromolecule of polyethylene glycol with molecular weight of 3000, 6000, and 10000 was used for measurement of the molecular weight cut off (MWCO). To measure the concentration of PEG solutions, spectrophotometry was employed at wavelength of 535 nm [35].

Rejection is a criterion accounting for the amount of the solute of interest in a solution retained by a selectively layer, i.e., the membrane. Indeed, the level of rejection of a substance represents the selective properties of a membrane towards that compound. It can be defined as follows:

$$R\% = \left(1 - \frac{C_p}{C_b}\right) \times 100 \quad (2)$$

C_p is the concentration of the substance of interest in the solution passing through the membrane and C_b is the concentration of the substance in the initial solution (feed solution).

In this research, rejection of 100-ppm solutions of mono and polyvalent salts as well as separation of the Direct yellow 12 dye ($C_{30}H_{26}N_4Na_2O_8S_2$; MW: 680.22 Da) with a concentration of 100 ppm were evaluated. The concentration of salt solutions was determined using conductivity of the dye concentration through spectrophotometry. Similarly, the effect of effective parameters such as pressure (1, 2, 3, and 4 bar), flow rate (2, 4, 6, 8 L/min), and pH (3, 7, 11) on the membrane separation process was further investigated.

2-6. Determination of Sulfonation Degree

Degree of sulfonation (DS) can be defined as the average number of sulfonic groups present in a sulfonated polymer. It is measurable through various methods including titration, NMR, FT-IR, and elemental analysis [30-32]. Here, titration was used for determination of DS. Since SPSf obtained from synthesis contains sulfonated groups in the form of sodium salt ($-SO_3^-Na^+$), to determine the sulfonation degree, 0.3 g of the polymer in 50 ml 2 M HCl solution was placed in an oven for 24 hours at 70 °C. Note that use of a concentrated solution along with suitable temperature and time causes the sulfonated groups to be converted from salt form to fully acidic forms ($-SO_3H$). Next, the polymer was washed profusely with water to fully remove HCl off the polymer. If washing is not performed properly, a huge error will occur during titration.

Thereafter, the polymer was placed in 40 ml sodium chloride 1 M salt for one day at ambient temperature in order for all protons (H^+) exchange ions with sodium (Na^+) and be liberated inside the solution. Each 10 ml of the solution was titrated with NaOH 0.01 M in the presence of one drop of phenolphthalein detector. To increase the accuracy of determination of sulfonation degree, titration was replicated three times.

To determine DS, first ion exchange capacity (IEC) should be calculated:

$$IEC = \frac{C_{NaOH} \times V_{NaOH}}{W_{dry}} \quad (3)$$

C_{NaOH} and V_{NaOH} are the concentration and volume of the NaOH solution used in the titration and W_{dry} is the weight of the utilized polymer. Now, using the calculated IEC, DS can be determined as follows:

$$DS = \frac{M_0 \times IEC}{1000 - 81 \times IEC} \quad (4)$$

M_0 is the weight of the replicating unit in the polymer equal to 442 g/mol the weight of the sulfonic group is 81 [36].

2-7. Measurement of the Water Absorption

To investigate the level of hydrophilicity of the synthesized membranes, the difference between the weights of wet in relation with dried membranes is used. The objective of this experiment was to measure the amount of water absorbed by each of the synthesized membranes. The membrane samples were placed in a vessel of distilled water for 24 hours. They were then weighed by a digital balance. Next, they were immediately placed in an oven with a temperature of 40 °C to lose their water gradually and reach a constant weight value. Finally, using the weight difference of the wet and dry membranes according to Eq. (5), the level of water absorption can be calculated [30-32].

$$\text{Water uptake} = \frac{W_{wet} - W_{dry}}{W_{wet}} \times 100(\%) \quad (5)$$

RESULTS AND DISCUSSION

We synthesized sulfonated polysulfone membranes (SPSf) by sulfonation agent TMSCIS. The effect of the degree of sulfonation was further investigated on formation of the membrane. To increase mechanical resistance, a combination of these membranes with a polysulfone membrane PSf was synthesized. Likewise, to develop the selectivity, TiO_2 nanoparticles were added to the optimal combination of PSf/SPSf membrane.

1. Synthesis of the Sulfonated Polysulfone Polymer

Sulfonation is adding sulfonic groups to the principal aromatic structure of PSf and PES. This is a electrophile aromatic substitution reaction in which one hydrogen atom is substituted with a sulfonic group [37]. Sulfonation of polysulfone was done according to the method presented in 2.2.2 To determine the degree of sulfonation, the titration method described in 2.2.6 was employed. The diagram of Fig. 2 demonstrates the volume of consumed NaOH for titrat ion of the sulfonated samples at different times. Based on the volume of the NaOH used in titration, degree of sulfonation was calculated using Eqs. (3) and (4), which results are displayed in Fig. 2.

As can be observed in Fig. 2, degree of sulfonation increases over time. Within times shorter than six hours, DS increases dramatically in a linear fashion over time, but within longer times, the slope drastically declines, suggesting that the rate of the sulfonation reaction decreases. This can be due to both reduced concentration of the sulfonation agent and presence of sulfonated groups onto the polymer rings, where increased ring resonance significantly decreases the tendency towards reaction [37]. Therefore, it seems that sulfonation time of six hours which is equal to 67% degree of sulfonation can be suitable as the optimal time for sulfonation operations in the next stages. This is because an average amount of DS is

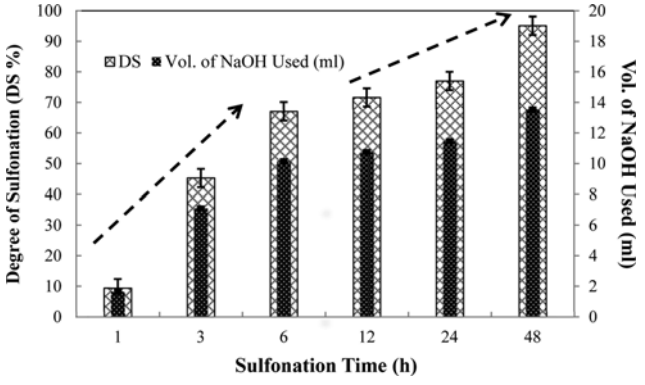

Fig. 2. The effect of sulfonation time on degree of sulfonation for PSf.

obtained during a short time, while it would not face the problem polymer swelling with high DS during membrane synthesis [38].

2. Synthesis of Membrane Using Sulfonated Polysulfone

Sulfonated polysulfone with high DS is widely used in the synthesis of ion exchange membranes in fuel cells. To achieve a membrane with an acceptable performance, SPSf with different degrees of sulfonation was used for membrane synthesis using phase inversion method. All of the synthesized membranes were highly fragile and heterogeneous, so they were not usable under high pressure and flow rate. Indeed, the presence of hydrophilic as well as sulfonated polarized groups onto the polysulfone chain, on the one hand, and dissociation of polymer chains along with reduction of its molecular weight, on the other, resulted in considerable increase in swelling, thus significantly reducing the mechanical resistance. Membrane synthesis in the section also clearly demonstrated that membrane swelling grows with increased sulfonation degree. Yet, the polymer sulfonated within six hours, which is equal to a sulfonation degree of 67.1% according to Fig. 2, has a lower level of swelling at an acceptable sulfonation degree.

Therefore, it seems that although connection of sulfonated groups with the PSf chains promises dramatic growth of hydrophilicity, it would not bring about the desired outcome from the point of view of membrane synthesis using phase inversion method. Thus, to synthesize resistant membranes out of SPSf using phase inversion method, a combination of this polymer with optimal DS (67%) with more resistant polymers such as raw polysulfone seems to be effective.

3. Synthesis of Sulfonated Polysulfone/Polysulfone Blended Membranes

The high swelling of the membranes synthesized with polymers enjoying high hydrophilicity such as SPSf is a serious problem in synthesizing membranes with fine and stable performance. Methods of cross-linking and mixing polymers such as polyurethane SPSF/(PU), polyethersulfone (SPSF/(PES)) and Sulfonated polyetheretherketone (SPEEK) and cellulose acetate SPSF/(CA) are among appropriate solutions widely used to overcome this problem and synthesized membranes with higher selectivity and rejection properties with longer durability. In this research, the combination of SPSf with a sulfonation degree of 67% with PSf was used to prepare blended membranes.

3-1. Determination of the Optimal SPSf to PSf Ratio in the SPSf/PSf Blended Membrane

To obtain the optimal blending percentage of the mix of these two polymers, their sum of the concentration to the solvent ratio was considered constant (25 wt%) and the SPSf/PSf ratio was altered. To evaluate the performance of the membrane and its performance sustainability over time, the distilled water flux passing through the membrane was also tested with its results provided in diagram 3 in Fig. 3.

As can be seen in Fig. 3, when the percentage of SPSf increases, so does the distilled water flux dramatically. This is due to presence of sulfonate polarized the groups within the membrane structure. They cause increased membrane selectivity with their high hydrophilicity property, on the one hand, and bring about increased repulsion between polysulfone chains within the membrane film structure and thus increased number of pores and size of superficial

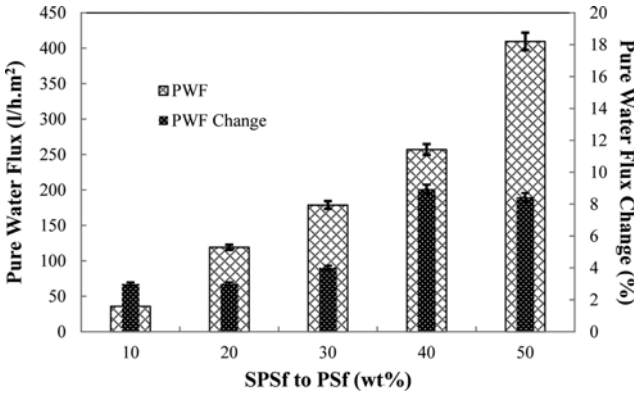

Fig. 3. The flux of membranes synthesized with different blending percentages of SPSf/PSf; primary water flux (PWF) and the changes in the flux after 15 min (PWF change).

pores, on the other hand [39]. In diagram 3, it is also noteworthy that as the SPSf percentage grows within the membrane structure, particularly up to 40 or 50%, variations of the flux develop as well suggesting instability of the filtration performance over time. This can be due to increased swelling of the membrane film and its low physical resistance. Since it is possible to control the size of membrane pores through changing other parameters of membrane synthesis, of greater significance is the drop in the mechanical resistance and stability of membranes throughout the process. Eventually, the membrane containing SPSf/PSf compound (30/70) was selected as the optimal percentage compound enjoying high flux, low swelling, and stable filtration performance with suitable replicability. For the rest of the research, for determination of the optimal value of other parameters, this ratio has been considered constant.

3-2. Determination of the Optimal Concentration of the Polymer in the SPSf/PSf Blended Membrane

One of the key parameters in synthesizing a membrane is the concentration of the polymer in the casting solution having the potential to significantly influence the final structure and thus performance of membranes. In this research, the effect of increasing the concentration of the PSf/SPSf polymeric compound from 26 to 32% on the performance of the synthesized membrane was evaluated. The results are provided in Fig. 4 in the form of water flux, flux, and percentage of separation of sodium sulfate salt.

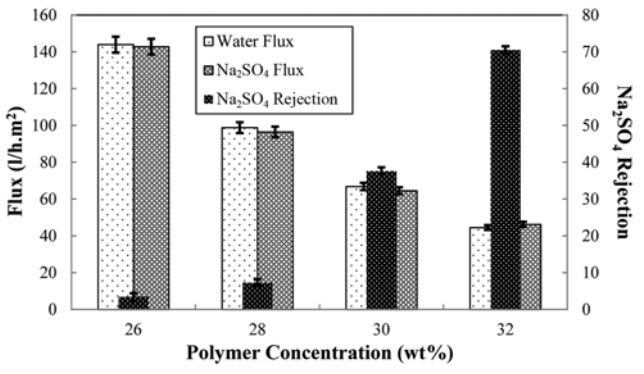

Fig. 4. The effect of the polymer concentration on the flux of distilled water, flux, and separation of the Na_2SO_4 solution.

In Fig. 4, as the concentration of the polymer increases, water flux decreases. In general, higher concentration of the polymer inside the solution causes the interface of the film and coagulation bath to become richer in polymer, resulting in lowered coagulation rate and delayed phase separation of the polymer film. Therefore, the thickness of the skin layer grows, while its porosity diminishes, generally followed by reduced flux and of course, in the majority of cases, elevated levels of membrane rejection. Furthermore, the flux of the salt solution passing through the membrane is well congruent with the results obtained from the distilled water flux test.

In terms of separation of sodium sulfate salt, as can be seen in Fig. 4, at higher concentrations of the polymer, rejection of the bivalent salt of sodium sulfate develops. It seems that as the polymer concentration increases, the size of pores diminish, while the presence of sulfonated polarized groups grows on the membrane surface as well as the external structure of the membrane pores due to increased SPSf concentration. Therefore, reduced pore size and elevated Donnan repulsion force lead to increased salt rejection. Note that at higher percentages of polymer (34%), due to extreme growth of the solution's viscosity, there was practically no possibility for formation of a homogeneous casting solution during long periods of time. Thus, elevation of the polymer concentration was done up to 32% and selected as the optimal solution for synthesis of a loose nanofiltration membrane with desirable performance.

3-3. Determination of the Optimal Temperature of the Coagulation Bath for Synthesis of SPSf/PSf Blended Membrane

Another influential parameter in formation of the structure, level of porosity, and the size of membrane pores is the temperature of the coagulation bath. Depending on the type of polymer and presence of functional groups available on the polymer chain, the effect of bath temperature can be significant or minor. The results obtained from investigating the effect of the temperature of coagulation bath (5, 15, and 25 °C) on the distilled water flux, flux, and rejection of the sodium sulfate bivalent salt are provided in Fig. 5.

As at the temperature of the coagulation bath declines, the phase inversion process between the solvent (NMP) and non-solvent (water) tends toward delayed separation. Accordingly, despite increased nucleation rate, their growth slows down, resulting in reduced average pore size. The outcome of this process is diminished distilled water flux and magnified percentage of membranes' rejection (Fig. 5).

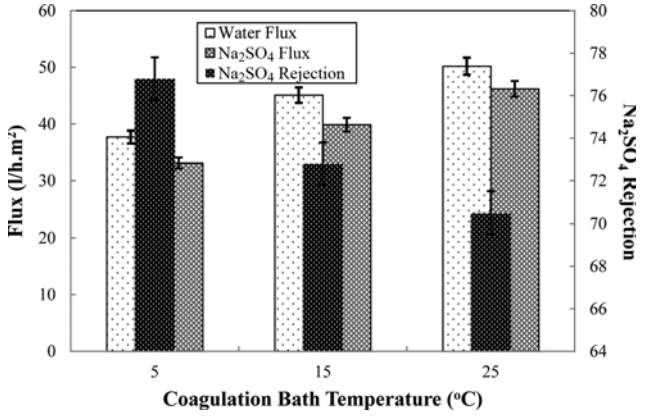

Fig. 5. The effect of coagulation bath temperature on the distilled water flux, flux, and separation of Na_2SO_4 solution.

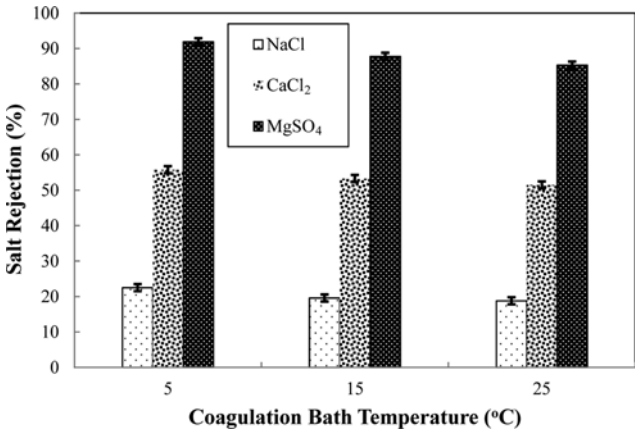

Fig. 6. The effect of coagulation bath temperature on the separation of $MgSO_4$, $CaCl_2$ and NaCl solution.

On the other side, the results indicate that variations of the flux and rejection of SPSf/PSs blended membranes, albeit being evident, is not very large because presence of sulfonated groups, due to bipolar-bipolar repulsion, causes the chains not be able to approach each other beyond a certain extent, and thus the size of pores would not decrease beyond a certain minimum value. Therefore, as the temperature in the bath diminishes by 20 °C, the extent of sodium sulfate rejection increases only by 6%. Hence, the average temperature of 15 °C was chosen as the optimal temperature in which salt retention behavior of synthesized membrane is acceptable. As clearly seen in Fig. 5 and Fig. 6, rejection of $MgSO_4$, Na_2SO_4, $CaCl_2$ and NaCl by nanofiltration membranes fabricated at coagulation bath with the temperature of 15 °C, is 19.6, 53.3, 72.8 and 87.8%, respectively.

The results show that synthesized membranes reject the various salts in proportion to their molecular size, so the order of rejection is simply: $MgSO_4$>Na_2SO_4>$CaCl_2$>NaCl.

4. Synthesis of SPSf/PSf Blended Membrane Containing Titanium Nanoparticles

TiO_2 nanoparticles with average particle size of 25 nm were loaded into structure of optimal membrane. Fig. 7 shows FESEM image and particle size distribution of nanoparticles measured by ImageJ software.

The presented SEM image and particle size distribution confirm that the approximate size of TiO_2 nanoparticle is 25 nm. The presence of TiO_2 nanoparticles within the structure and especially the membrane surface has multiple effects. On one hand, TiO_2 nanoparticles bring about reduced pore size and flux by establishing hydrogen and dipolar bonds between the polymer chains. On the other, it causes increased membrane hydrophilicity and increased flux. Incidence of each of these aforementioned events is contingent upon the concentration of TiO_2 nanoparticles loaded within the structure [24].

4-1. Investigation of the Effect of TiO_2 Nanoparticles on the Membrane Properties

The effect of the concentrations of 0.01, 0.05, and 0.1 wt% TiO_2 on the flux and rejection of the optimal nanofiltration membranes

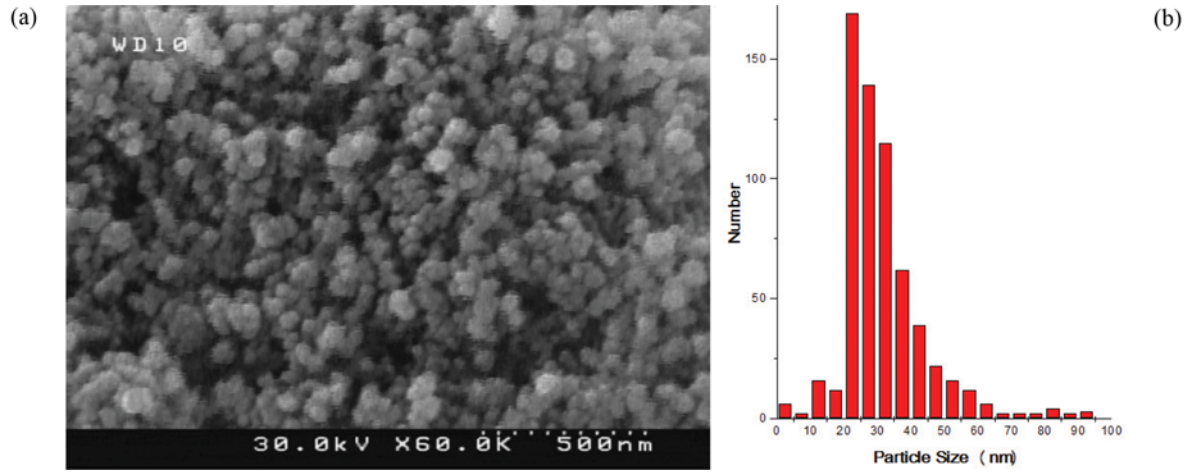

Fig. 7. FESEM image of TiO_2 nanoparticle (a) and size distribution of nanoparticles (b).

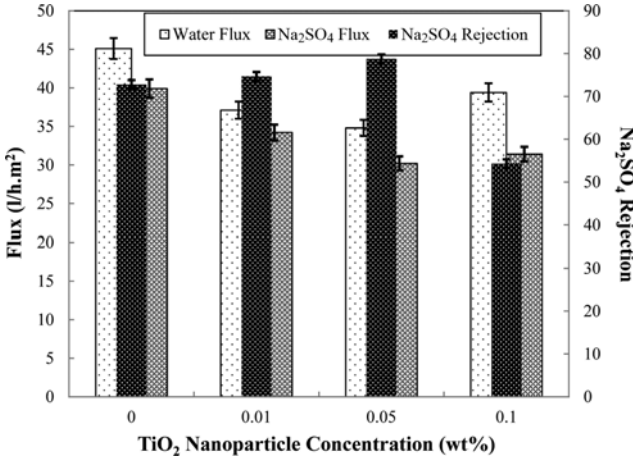

Fig. 8. The effect of the concentration of TiO_2 nanoparticles on the distilled water flux, flux, and separation of Na_2SO_4 solution.

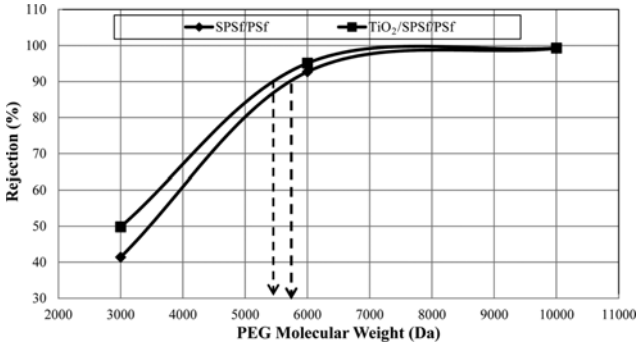

Fig. 9. Molecular weight cut off (MWCO) of sulfonated polysulfone membranes in the presence and the absence of TiO_2 nanoparticles.

synthesized in the previous stages was examined. The results are demonstrated in Fig. 8.

As can be observed in Fig. 8, at concentrations of 0.01 and 0.05 wt% TiO_2 the flux drops and, in turn, rejection grows. Therefore, at these concentrations, the effect of diminished pore size overrides elevated hydrophilicity, resulting in lowered flux and developed rejection of nanofiltration membranes. To ensure the alteration of pore sizes in the presence and absence of nanoparticles, the molecular weight cut off (MWCO) of TiO_2/SPSf/PSf and SPSf/PSf membranes was measured in the presence of TiO_2 0.05 wt% with its results indicated in Fig. 9. The molecular weight cut off (MWCO) of nanofiltration membranes is 5700, while for the nanofiltration membranes in the presence of TiO_2 nanoparticles is around 5300. According to the equation reported by Causserand et al. [40], the membrane mean pore size was determined as 3.3 nm for SPSf/PSf blended membrane and 3.2 nm for TiO_2/SPSf/PSf nanocomposite membrane. As previously mentioned, this size of pores diminishes in the presence of TiO_2 nanoparticles.

Indeed, it seems that considering high hydrophilicity of the surface of SPSf/PSf blended membranes resulting from the presence of sulfonated groups on to the membrane surface, the presence of TiO_2 nanoparticles within this low concentration range (0.01-0.05) would not play an important role in increasing the membrane's hydrophilicity. At higher percentages of TiO_2, the effect of hydrophilicity development is dominant; however, with even minor elevation of flux, the rejection of membranes declines. Therefore, the best filtration behavior is observed for nanocomposite membranes containing TiO_2 0.05 wt% enjoying water flux of 34 L/hm^2 and rejection of 78% for sodium sulfate.

5. Structural and Operational Comparison of SPSf/PSf Blended Membrane and the TiO_2/SPSf/PSf Nanocomposite Membrane

To achieve a loose nanofiltration membrane with acceptable performance, in the previous stages of the research, the sulfonated polysulfone polymer was fabricated and its DS was optimized. Optimal SPSf was used for synthesis of the SPSf/PSf blended membrane, followed by determination of the optimal ratio of the two polymers. This optimal ratio was employed, after which the membrane fabrication parameters including the polymer concentration and the coagulation bath temperature was investigated with their optimal value being specified. The optimal blended membrane was utilized for synthesis of a nanocomposite membrane containing TiO_2 nanoparticles, where the optimal concentration of the nanoparticles was determined for synthesis of the nanocomposite membrane. In this

Table 2. The list of the peaks present in FTIR analysis of PSf and SPSf samples and the causing agent of each peak

Causing agent of each peak	Peak frequency (cm^{-1})
Stretching vibration corresponding to the -OH group	3200-3600
Symmetric and asymmetric stretching vibration corresponding to the methyl group	3065
	2967
Stretching vibration corresponding to the aromatic C=C group	1584
	1484
Shape change in the asymmetric C-H bond of the methyl group	1406
Shape change in the symmetric C-H bond of the methyl group	1365
Symmetric stretching vibration corresponding to O=S=O group of sulfone	1325
	1296
Asymmetric stretching vibration corresponding to C-O-C group of Aryl ether	1241
Asymmetric stretching vibration corresponding to O=S=O group of sulfonate	1170
Symmetric stretching vibration corresponding to O=S=O group of sulfone	1145
Vibration corresponding to aromatic ring	1099
Symmetric stretching vibration corresponding to O=S=O group of sulfonate	1027
Stretching vibration corresponding to Ti-O group	841

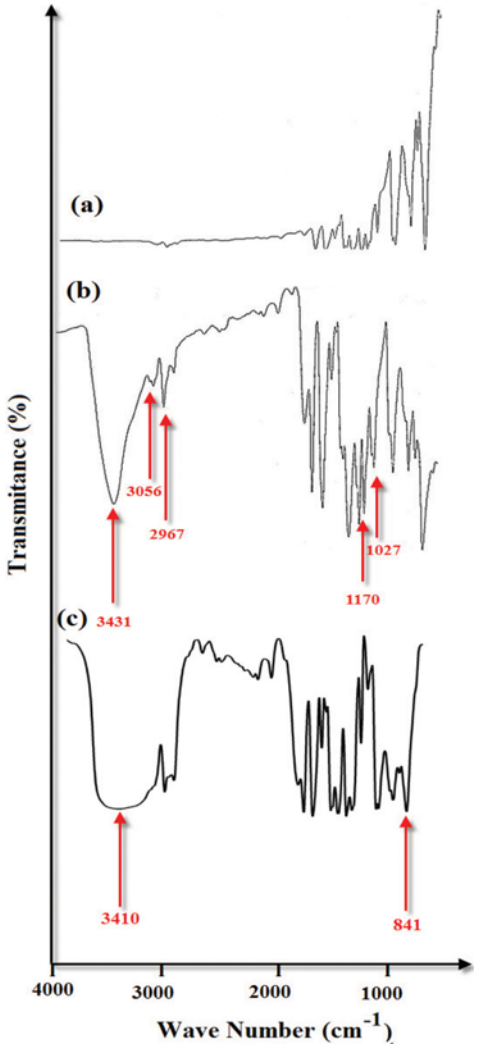

Fig. 10. FTIR spectra of raw polysulfone membrane (a) and sulfonated polysulfone membrane (b) and sulfonated polysulfone membrane containing TiO_2 nanoparticles (c).

section is performed the structural (chemical structure of the surface, surface hydrophilicity, surface morphology, and the cross-section structure) and functional (filtration of water, salt solution and the dye solution) comparison of the optimal membrane belonging to the gtoup of SPSf/PSf blended and TiO_2/SPSf/PSf nanocomposite membranes.

5-1. Comparison of the Chemical Structure of TiO_2/SPSf/PSf and SPSf/PSf Membranes Using Infrared Spectrophotometry

To compare the chemical structure of the surface of the studied membranes, FT-IR analysis was done on raw and sulfonated polysulfone samples together with the nanocomposite membrane, results of which are provided in Table 2 and Fig. 10.

The analysis results clearly demonstrate the presence of sulfonate groups in the PSf chain after the sulfonation reaction. The peaks at 1,170 and 1,027 cm^{-1} are attributed to symmetrical and asymmetrical stretching vibrations of the sulfonate groups. Furthermore, the presence of a peak at 3,200-3,600 cm^{-1} represents the stretching vibrations of the -OH group. Other properties of the SPSf and PSf peaks are provided in Table 2. In a similar vein, considering the spectra of the nanocomposite membrane, the peaks at 3410 and 841 are related to the stretching vibrations of the superficial -OH group and the Ti-O group of TiO_2 nanoparticles, respectively, confirming the presence of nanoparticles within the membrane structure.

5-2. Comparison of the Morphology of the Surface of TiO_2/SPSf/PSf Membranes Using AFM Analysis

To compare the morphology of the surface of the synthesized membranes and recognize the effects of the synthesis method on parameters such as surface roughness, AFM analysis was conducted on the surface of TiO_2/SPSf/PSf, APSf/PSf, and PSf membranes. The results are provided in Table 3.

As is evident from the analysis results, sulfonation and addition of nanoparticles elevate the surface roughness. The roughest surface belongs to the nanocomposite membrane, possibly due to presence of nanoparticles on the membrane surface. Indeed, the hydrophilicity of nanoparticles causes to move towards the coagulation bath during the phase inversion process and be trapped within the mem-

Table 3. Three-dimensional images of AFM and the roughness values of the synthesized membranes

Membrane type	3D AFM image	Roughness		
		Peak to valley	Mean	RMS
PSf	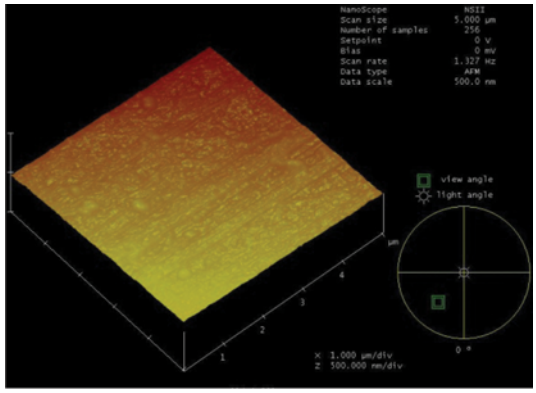	96	57	8.1
SPSf/PSf	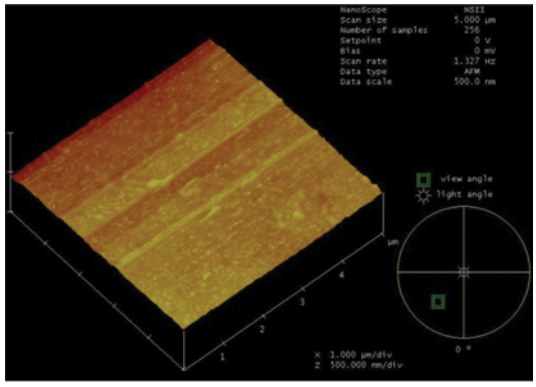	156	83	12.6
TiO_2/SPSf/PSf	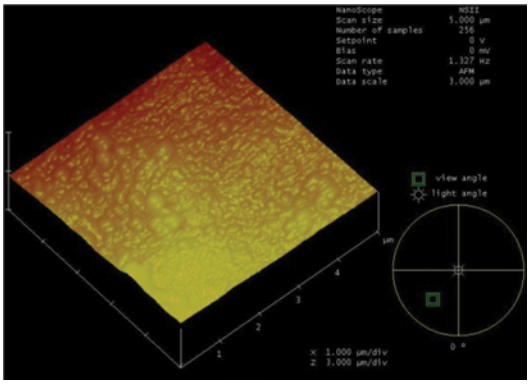	325	91	59.5

brane superficial layer, resulting in increased surface roughness of the nanocomposite membranes [17,41].

5-3. Comparison of the Surface Structure and Cross-section of the TiO_2/SPSf/PSf and SPSf/PSf Membranes Using SEM Analysis

Fig. 11 demonstrates the scanning electron microscopy images of the surface and cross-section of the TiO_2/SPSf/PSf, SPSf/PSf, and PSf membranes. As is evident from the images, the surface of PSf membranes is totally smooth, while the membrane surface seems slightly rougher after sulfonation, though is still homogeneous and smooth. Confirming the AFM results, the obtained results in this section reveal that the surface becomes totally rough and uneven in the presence of TiO_2 nanoparticles. It seems that this is due to presence of nanoparticles within the membrane structure significantly influencing the surface roughness. This has also been observed by other researchers [42,43].

SEM images of the cross-section of membranes represent alteration of the membrane structure before and after sulfonation and the effect of adding TiO_2 nanoparticles. As can be observed from Fig. 11, in the PSf membrane, finger-like pores are located right after the upper compressed layer, where past these pores is a thick sponge-like layer. This lower thick sponge-like layer significantly reduces the membrane flux due to low porosity; however, in the two PSf/SPSf membranes in the presence and absence of TiO_2, the general structure of asymmetrical membranes remains fully intact. This structure consists of three layers: the upper compressed layer, sponge layer, and finger layer. Presence of this structure represents mem-

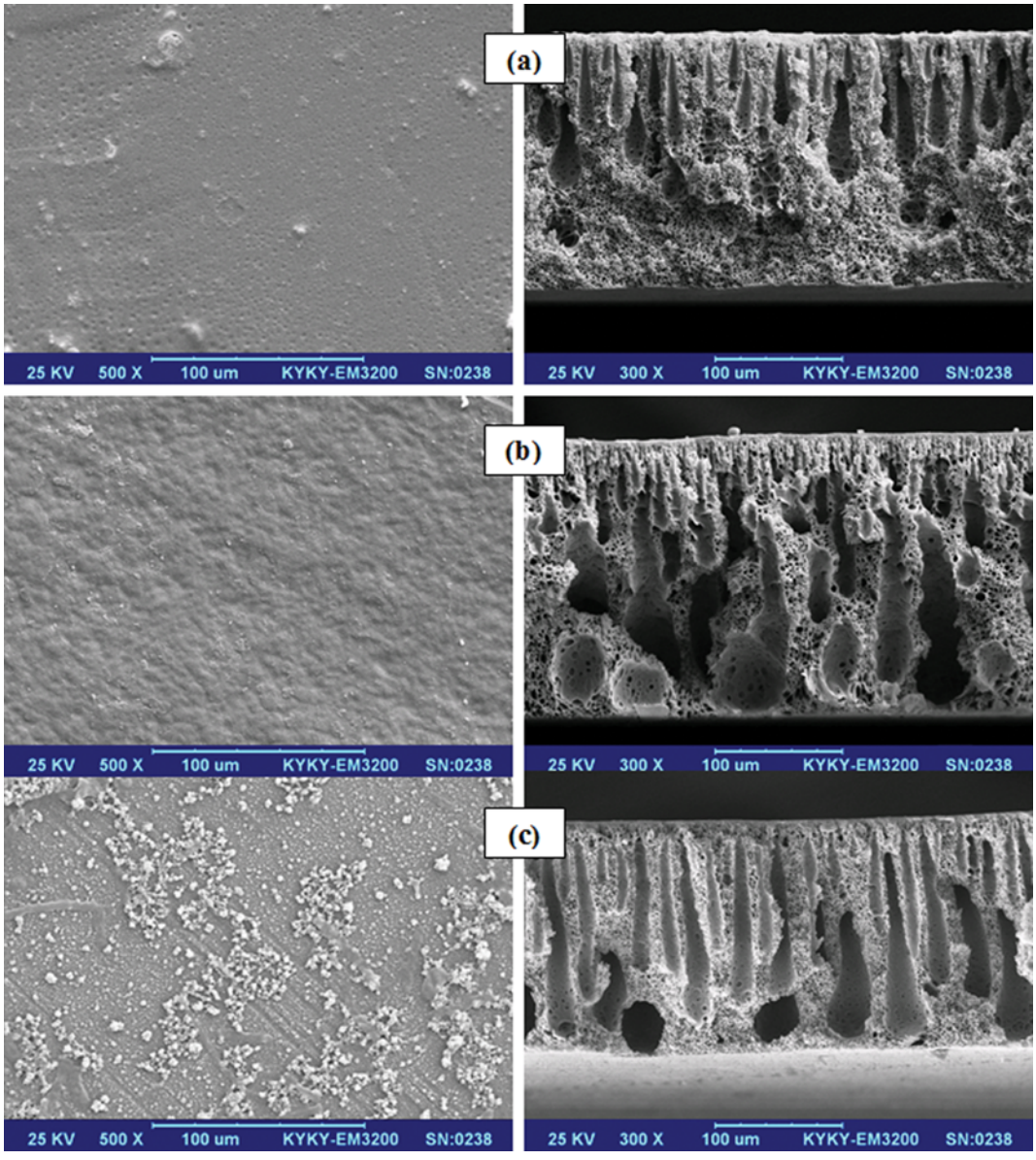

Fig. 11. Surface (left) and cross section (right) SEM images of the raw polysulfone membrane (a), sulfonated polysulfone membrane (b), and sulfonated polysulfone membrane containing TiO_2 nanoparticles.

branes with higher performance that require lower pressure and show less fouling. Indeed, the lower finger-like layer of these membranes enhances the membrane flux while retaining the mechanical resistance.

From the cross-sectional images of the SPSf membranes in the presence and absence of TiO_2 nanoparticles, it is also deducible that the size of pores has reduced in the presence of nanoparticles. As previously stated, in the presence of nanoparticles, the chains approach each other within the polymer matrix due to the hydrogen and dipolar bonds between the sulfonate groups and nanoparticles, resulting in lowered membrane pore size.

5-4. Comparison of Water Absorption by the SPSf/PSf Blended Membranes and the TiO_2/SPSf/PSf Membranes

The competence of water absorption is a key property of SPSf making them usable in many fields such as water purification and fuel cells. To compare the level of hydrophilicity of the nanofiltration membranes synthesized under various conditions, the amount of water absorption by these membranes was described, measured and reported. The results are shown for the SPSf/PSf blended membrane in the presence and absence of TiO_2 in Fig. 12. The highest water absorption belongs to the SPSf/PSf membranes. Water absorption is highly dependent on the sulfonic acid content, where the membrane water absorption level is in direct relationship with the sulfonation degree. This is because sulfonic acid groups are hydrophilic, thus the hydrophilic ionic areas might develop large and continuous channels, resulting in increased water absorption capacity. Therefore, membranes with higher sulfonation degree can absorb more water [44].

On the other hand, as evident from the data in Fig. 12, membranes absorb less water in the presence of TiO_2 nanoparticles due

to increased number of cross-links and reduced porosity and size of the pores. As previously mentioned, it seems that TiO_2 nanoparticles play their major role in reducing the size of membrane pores within the concentration range used in this research rather than influencing the surface hydrophilicity. Therefore, as also observable from the results of molecular weight cut off (MWCO) (Fig. 9), TiO_2 nanoparticles cause diminished pore size, whereby they show lower water absorption levels (Fig. 12).

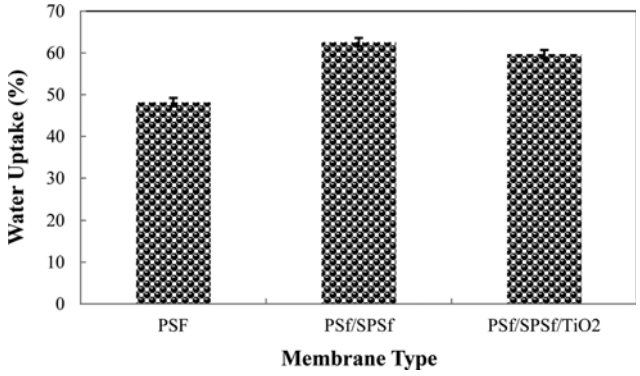

Fig. 12. Percentage of water absorption by the raw polysulfone membrane, sulfonated polysulfone membrane, and sulfonated polysulfone membrane containing TiO_2 nanoparticles.

5-5. Comparison of the Filtration Behavior of the SPSf/PSf Blended Membrane and that of the TiO_2/SPSf/PSf Nanocomposite Membrane in Separation of Textile Dyes Out of Water

To compare the performance of the synthesized loose nanofiltration membranes, flux variation, and the level of rejection, 100-ppm solution of the direct yellow 12 dye was evaluated over time. The results are illustrated in Fig. 13.

As can be observed, although both membranes present a desirable performance in separating the Direct yellow 12 dye, the blended membranes containing TiO_2 nanoparticles have a lower flux and higher rejection. Direct yellow 12 has two sulfonate groups (see Table 1). At pHs above 2 these sulfonate groups convert to their anionic form. Therefore, surface charge of Direct yellow 12 at filtration medium is negative. On the other side TiO_2 nanoparticles with pH_{PZC} about 6.2-7 [45], have negative superficial charge in the pH>7. Therefore, dye rejection of TiO_2/SPSf/PSf nanocomposite membrane is more than SPSf/PSf membrane. This is due to lower average diameter of the pores and more effective superficial charge from TiO_2 nanoparticles.

In addition, the effect of parameters such as operational pressure, the flow rate, and the acidity of the filtration environment on the performance of these membranes was also investigated. The examination of the effect of pressure on flux and rejection of the membranes in the presence and absence of TiO_2 nanoparticles indicated that as the pressure rises, so does the flux passing through

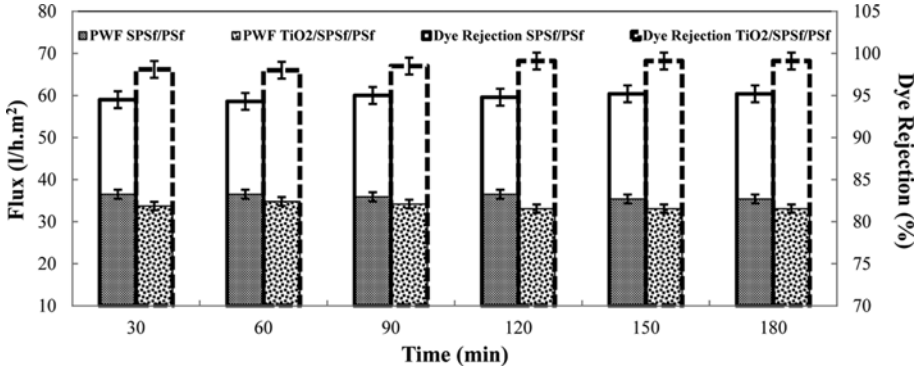

Fig. 13. Flux and rejection of the dye solution by the sulfonated polysulfone membrane and sulfonated polysulfone membrane containing TiO_2 nanoparticles.

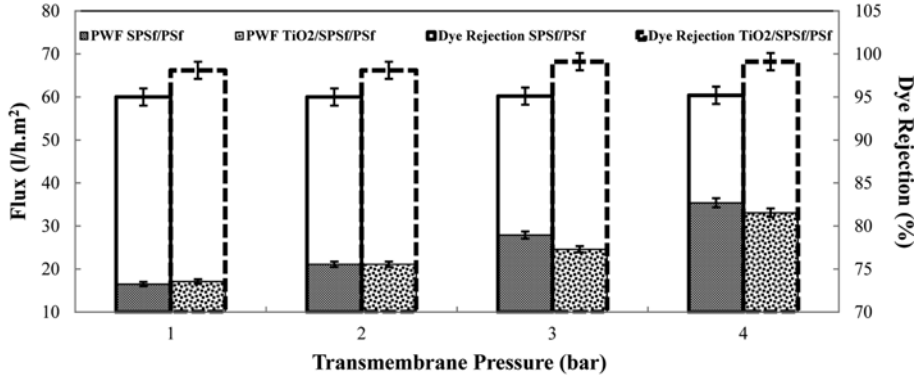

Fig. 14. The effect of pressure on the level of flux and rejection of the sulfonated polysulfone membrane and sulfonated polysulfone membrane containing TiO_2 nanoparticles.

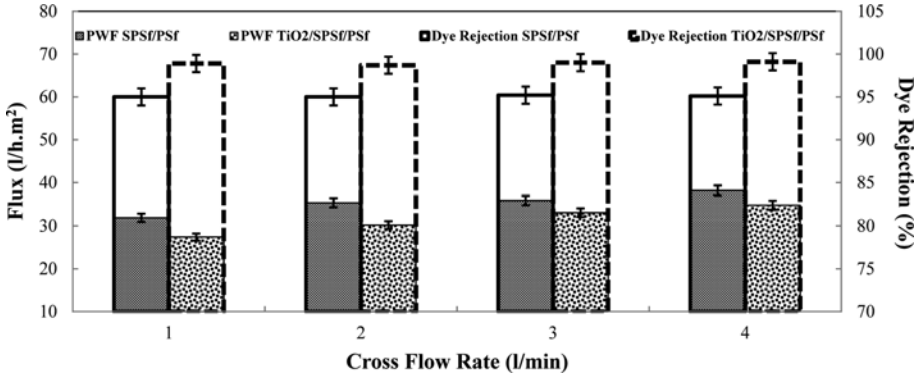

Fig. 15. The effect of flow rate on the flux and rejection levels of the sulfonated polysulfone membrane and sulfonated polysulfone membrane containing TiO_2 nanoparticles.

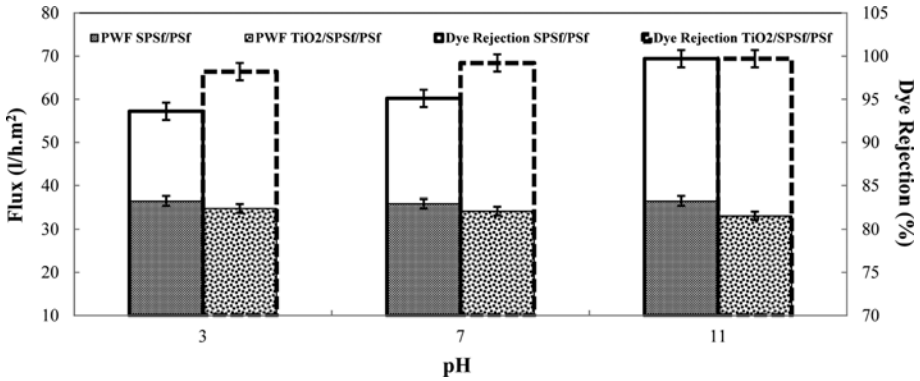

Fig. 16. The effect of pH on the level of flux and rejection of the sulfonated polysulfone membrane and sulfonated polysulfone membrane containing TiO_2 nanoparticles.

the membrane, while the level of rejection remains almost constant.

As can be observed from Fig. 14, when the operational pressure grows from 1 to 4 bars, the flux reaches 35.5 L/m^2·h from 16.5 L/m^2·h in the absence and 33.1 L/m^2·h from 17.1 L/m^2·h in the presence of TiO_2 nanoparticles. Whereas, the dye rejection still remains unchanged. This brings promise of the possibility of using nanocomposite membranes at low operational pressure with acceptable permeability.

The effect of flow rate on the flux and rejection levels of the dye was also studied. From Fig. 15, as the flow rate grows, the flux shows an ascending trend possibly due to diminished concentrative polarization on the surface of membranes at higher feed flow rates.

Based on the results provided in Fig. 15, increased flow rate from 1 to 4 L/min elevates the SPSf/PSf flux and TiO_2/SPSf/PSf nanocomposite membrane by 19 and 27%, respectively. It seems that in the presence of nanoparticles the concentration polarization layer has a lower resistance. In response to this, when the flow rate grows, the resistance of this layer declines, resulting in increased flux.

The effect of variations of pH on the level of rejection of the Direct yellow 12 dye was also investigated. The results are shown in Fig. 16.

As can be seen from the figure, as the pH of the filtration environment increases the amount of flux remains almost constant. However, considering the level of salt rejection, at alkaline pHs the negative charge of the membrane surface reaches its maximum and the studied dye totally converts into a di-anion. Therefore, the repulsion reaches its maximum, resulting in increased level of rejection. At acidic pHs also, although the level of rejection is acceptable, due to diminished Donnan repulsion force between the membrane surface and the dye, declining levels of rejection can be clearly observed. The similar behavior was observed in salt rejection at different pHs of feed solution. As presented in Fig. 17 any increase in pH enhances salt rejection of NaCl and Na_2SO_4 while diminishes

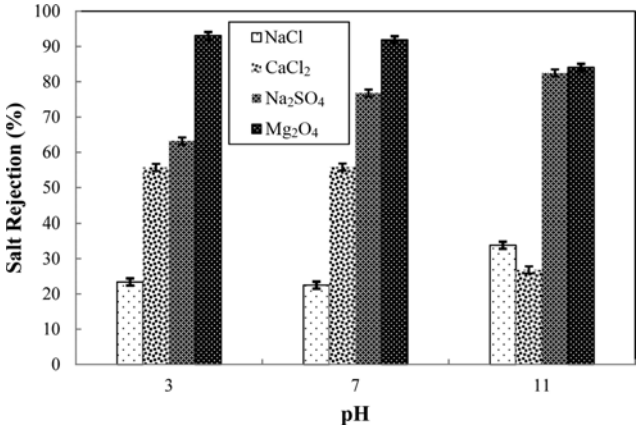

Fig. 17. The effect of pH on the salt rejection of the synthesized loose nanofiltration membranes.

salt retention of $CaCl_2$ and $MgSO_4$. It seems that at alkaline pH, sulfonated groups convert to their anionic forms, which makes membrane surface negatively charged. This phenomenon enhances salt rejection of mono (Cl^-) and divalent (SO_4^{2-}). In contrast at acidic pHs, sulfonate groups convert to their cationic form, which increases positive charge of membrane surface and enhances salt rejection of divalent cations (Ca^{2+} and Mg^{2+}).

Note that the dominant mechanism in salt rejection is Donnan repulsion rather than size exclusion; therefore, no difference was observed between salt rejection behavior of SPSf/PSf and SPSf/PSf/TiO_2 membrane.

Considering all characteristics of synthesized membrane especially MWCO, pure water flux, salt rejection and dye separation, the fabricated SPSf/PSf and TiO_2/SPSf/PSf belong to the nanofiltration category of membrane, namely, loose nanofiltration membrane, which are high flux, low pressure drop membranes that have good performance in salt rejection and NOM separation [29].

CONCLUSION

The main objective of this study was the preparation and fabrication of loose nanofiltration membranes with high flux, resistance against fouling, and applicability in high filtration flow rates and low operational pressure for separation of dyes from textile wastewater. Four main steps were taken in this project with their findings listed below:

At the sulfonation of polysulfone stage, SPSf with a degree of sulfonation of 67% was selected as the optimal structure.

At the SPSf/PSf blended membrane synthesis stage, the 30/70 weight ratio of SPSf/PSf was determined as the optimal ratio for fabrication of the blended membrane.

At the membrane synthesis optimization step, a concentration of 32 wt% of the polymer and 15 °C coagulation bath temperature were chosen as the optimal parameters of membrane synthesis.

At the TiO_2/SPSf/PSf nanocomposite membrane synthesis step, the nanocomposite membrane containing 0.05 wt% of the nanoparticles was chosen as the optimal membrane.

Finally, the structure and performance of the TiO_2/SPSf/PSf, SPSf/PSf, and PSf membranes were compared. Based on the results, the SPSf/PSf membranes enjoy the highest hydrophilicity, promising their usability for fuel cells. The TiO_2/SPSf/PSf nanocomposite membranes enjoy the highest surface roughness, the smallest pore size, the highest level of rejection and the lowest level of fouling, having the potential to be utilized at low operational pressure and high filtration rate.

REFERENCES

1. C. Tang and V. Chen, *Desalination*, **143**, 11 (2002).
2. M. S. Nawaz and M. Ahsan, *Alexandria Eng. J.*, **53**, 717 (2014).
3. W.-J. Lau and A. F. Ismail, *Desalination*, **245**, 321 (2009).
4. J. Lin, W. Ye, H. Zeng, H. Yang, J. Shen, S. Darvishmanesh, P. Luis, A. Sotto and B. Van der Bruggen, *J. Membr. Sci.*, **477**, 183 (2015).
5. A. W. Mohammad, Y. H. Teow, W. L. Ang, Y. T. Chung, D. L. Oatley-Radcliffe and N. Hilal, *Desalination*, **356**, 226 (2015).
6. Y. Liu, S. Zhang, Z. Zhou, J. Ren, Z. Geng, J. Luan and G. Wang, *J. Membr. Sci.*, **394-395**, 218 (2012).
7. A. Akbari, S. Desclaux, J. C. Rouch, P. Aptel and J. C. Remigy, *J. Membr. Sci.*, **286**, 342 (2006).
8. T. Chidambaram, Y. Oren and M. Noel, *Chem. Eng. J.*, **262**, 156 (2015).
9. B. Van der Bruggen, G. Cornelis, C. Vandecasteele and I. Devreese, *Desalination*, **175**, 111 (2005).
10. C.-H. Yu, C.-H. Wu, C.-H. Lin, C.-H. Hsiao and C.-F. Lin, *Sep. Purif. Technol.*, **64**, 206 (2008).
11. D. Möckel, E. Staude and M. D. Guiver, *J. Membr. Sci.*, **158**, 63 (1999).
12. N. Maximous, G. Nakhla and W. Wan, *J. Membr. Sci.*, **339**, 93 (2009).
13. L. Braeken, K. Boussu, B. Van der Bruggen and C. Vandecasteele, *ChemPhysChem*, **6**, 1606 (2005).
14. M. R. Mehrnia, Y. M. Mojtahedi and M. Homayoonfal, *Desalination*, **372**, 75 (2015).
15. V. Kochkodan, D. J. Johnson and N. Hilal, *Adv. Colloid Interface Sci.*, **206**, 116 (2014).
16. Y. Mansourpanah, A. Kakanejadifard, F. Dehrizi, M. Tabatabaei and H. Afarani, *Korean J. Chem. Eng.*, **32**, 149 (2015).
17. M. Homayoonfal, M. R. Mehrnia, M. Shariaty-Niassar, A. Akbari, A. F. Ismail and T. Matsuura, *Desalination*, **354**, 125 (2014).
18. W. Sun, J. Liu, H. Chu and B. Dong, *Membranes*, **3**, 226 (2013).
19. A. Akbari, Z. Derikvandi and S. M. Mojallali Rostami, *J. Ind. Eng. Chem.*, **28**, 268 (2015).
20. A. Akbari, E. Aliyarizadeh, S. M. Mojallali Rostami and M. Homayoonfal, *Desalination*, **377**, 11 (2016).
21. M. Homayoonfal, A. Akbari and M. R. Mehrnia, *Desalination*, **263**, 217 (2010).
22. L. Y. Ng, A. W. Mohammad, C. P. Leo and N. Hilal, *Desalination*, **308**, 15 (2013).
23. J. Kim and B. Van der Bruggen, *Enviror. Pollut.*, **158**, 2335 (2010).
24. M. Homayoonfal, M. R. Mehrnia, Y. M. Mojtahedi and A. F. Ismail, *Desalin. Water Treat.*, **51**, 3295 (2013).
25. L. Yu, Y. Zhang, Y. Wang, H. Zhang and J. Liu, *J. Hazard. Mater.*, **287**, 373 (2015).
26. Y. Wang, J. Zhu, G. Dong, Y. Zhang, N. Guo and J. Liu, *Sep. Purif. Technol.*, **150**, 243 (2015).
27. L. Yu, Y. Zhang, H. Zhang and J. Liu, *Desalination*, **359**, 176 (2015).
28. M. D. Afonso, *Desalination*, **191**, 262 (2006).
29. C. J. D. Fell, in: D. N. Richard, S. A. Stern (Eds.), Membrane Science and Technology, Elsevier, 113 (1995).
30. Y. Z. Fu and A. Manthiram, *J. Power Sources*, **157**, 222 (2006).
31. F. Lufrano, V. Baglio, P. Staiti, A. S. Arico' and V. Antonucci, *J. Power Sources*, **179**, 34 (2008).
32. R. Pedicini, A. Carbone, A. Saccà, I. Gatto, G. Di Marco and E. Passalacqua, *Polym. Test.*, **27**, 248 (2008).
33. J.-H. Kim and K.-H. Lee, *J. Membr. Sci.*, **138**, 153 (1998).
34. B. Chakrabarty, A. K. Ghoshal and M. K. Purkait, *J. Membr. Sci.*, **309**, 209 (2008).
35. A. D. Sabde, M. K. Trivedi, V. Ramachandhran, M. S. Hanra and B. M. Misra, *Desalination*, **114**, 223 (1997).
36. C. Lixon Buquet, F. Hamonic, A. Saiter, E. Dargent, D. Langevin and Q. T. Nguyen, *Thermochim. Acta*, **509**, 18 (2010).
37. C. Iojoiu, M. Maréchal, F. Chabert and J. Y. Sanchez, *Fuel Cells*, **5**,

344 (2005).
38. Y. Gao, G. P. Robertson, M. D. Guiver and X. Jian, *J. Polym. Sci., Part A: Polym. Chem.*, **41**, 497 (2003).
39. C. Manea and M. Mulder, *J. Membr. Sci.*, **206**, 443 (2002).
40. C. Causserand, S. Rouaix, A. Akbari and P. Aimar, *J. Membr. Sci.*, **238**, 177 (2004).
41. M. Homayoonfal, M. R. Mehrnia, S. Rahmani and Y. Mohades Mojtahedi, *J. Ind. Eng. Chem.*, **22**, 357 (2015).
42. F. Halek, S. Farahani and S. Hosseini, *Korean J. Chem. Eng.*, **32**, 1 (2015).
43. N. Rakhshan and M. Pakizeh, *Korean J. Chem. Eng.*, **32**, 2524 (2015).
44. Y. Devrim, S. Erkan, N. Baç and I. Eroğlu, *Int. J. Hydrogen Energy*, **34**, 3467 (2009).
45. X. Zhu, PhD Thesis, University of Oklahoma, 152 (2007).